IEEE Access
Multidisciplinary : Rapid Review : Open Access Journal

Received February 12, 2020, accepted February 20, 2020, date of publication February 28, 2020, date of current version March 11, 2020.

Digital Object Identifier 10.1109/ACCESS.2020.2977278

A New Geometric-Oriented Minimum-Energy Perfect Control Design in the IMC-Based State-Space Domain

WOJCIECH PRZEMYSŁAW HUNEK AND TOMASZ FELIKS
Institute of Control Engineering, Opole University of Technology, 45-758 Opole, Poland
Corresponding author: Wojciech Przemysław Hunek (w.hunek@po.edu.pl)

ABSTRACT A new geometric approach providing the minimum-energy issue for inverse model control-related perfect regulation of linear time-invariant multi-input/single-output plants described in the discrete-time state-space framework is proposed in the paper. Recent results have shown that the minimum-norm T-inverse does not guarantee the minimum-energy perfect control design, which has been confirmed by heuristic studies only. The new proposal, postulated throughout the manuscript, certifies the potential of nonunique σ-inverse regarding the minimum-energy behavior of inverse model control-based structures. After application of the proposed geometric approach dedicated to some class of state-space systems, we can precisely calculate the total energy of the multivariable perfect control runs. Thus, the analytical new methodology allows to obtain the minimum-energy inverse model control schemes, what constitutes the main accomplishment of the paper. Additionally, the aim of future analytical exploration covering the entire class of right-invertible state-space systems is clearly focused.

INDEX TERMS Geometric solution, perfect control, minimum-energy problem, inverses of nonsquare matrices, discrete-time state-space domain, LTI MIMO.

I. INTRODUCTION

The perfect control strategy, i.e. the deterministic case of the minimum variance control algorithm, is an attractive method due to its valuable properties [1]–[7]. For single-input/single-output or square systems, i.e. plants with the same number of input and output variables, the discussed control law may cause detrimental effects often leading to the damage a number of technological devices [8]–[25]. However, in the case of examination of nonsquare MIMO systems with different number of input and output signals, we can effectively impact the robustness of the IMC-related perfect control schemes. It can only be done for right-invertible plants described by both input-output and state-space LTI multivariable frameworks [26]–[28]. The higher number of input than output runs of nonsquare MIMO systems guarantees possibility of influencing this intriguing control law. Through an application of nonunique right generalized inverses of nonsquare parameter/polynomial matrices incorporated into the control plant description, the stability and minimum-energy behavior of the control inputs can be managed in the heuristic and analytical ways [29]. However, while the heuristic approach seems to be rather not to complex, the analytical approach is more difficult to solve. It should be emphasized, that the broadly known Moore-Penrose minimum-norm T-inverse does not provide the minimum-energy of the perfect control input runs, for instance see [4]. Notwithstanding, the formal analytical proof has not been given, up to now. Following the newly obtained results in this matter, the crucial ones are presented for the control community in the manuscript. Henceforth, the new analytical method based on a geometric approach, allowing to obtain the minimum-energy perfect control design for a special selected set of systems, gives rise to the introduction of the general minimum-energy perfect control theory in the nearest future. To recapitulate, through the application of the new analytical formula, we can correctly calculate the energy of the inverse model control schemes, finally to obtain the optimal instances. Thus, the simple elegant tool, arranging the degrees of freedom of the generalized σ-inverse, constitutes the new issue clearly outperforming the less accurate heuristic approaches.

The associate editor coordinating the review of this manuscript and approving it for publication was Nasim Ullah.

The paper is organized in the following manner. In Section II the preliminaries are given. Next section covers the methodology of the state-space perfect control design with application of generalized right σ-inverse. The perfect control energy problem with new corresponding issues provide the introduction of general theory in Section V. Simulation example of Section VI confirms the advantage of new proposed approach. In the end, the final conclusions and open problems are indicated.

II. PRELIMINARIES

Below the main mathematical symbols and abbreviations associated with the manuscript are tabelarized in order to eliminate any possible confusions.

$\mathbf{A}$, $\mathbf{B}$, $\mathbf{C}$, $\mathbf{D}$, $\mathbf{F}$, $\mathbf{J}$, β	– parameter matrices,
d	– time delay of a plant,
E_u	– energy of the perfect control input variables,
$\underline{\mathbf{G}}(q^{-1})$, $\underline{\beta}(q^{-1})$	– polynomial matrices in q^{-1},
$\mathbf{I_n}$	– identity n-matrix,
i	– index,
$\frac{L(\cdot)}{M(\cdot)}$	– rational function,
N	– time horizon,
q^{-1}	– backward shift operator,
z	– complex operator,
$z_{\mathbb{R}}$	– real number,
det(.)	– determinant symbol,
eig(.)	– eigenvalue symbol,
ker(.)	– kernel symbol,
Tr(.)	– matrix trace symbol,
$(.)^{\mathrm{R}}$	– (non)unique right inverse,
$(.)^{\mathrm{T}}$	– transpose symbol,
$\|.\|^2$	– norm symbol,
DOFs	– degrees of freedom,
IMC	– inverse model control,
LTI	– linear time-invariant,
MIMO	– multi-input/multi-output,
MISO	– multi-input/single-output,
MVC	– minimum variance control,
$S(\mathbf{A}, \mathbf{B}, \mathbf{C})$	– state-space plant.

III. PERFECT CONTROL LAW IN THE STATE-SPACE DOMAIN

Consider an LTI MIMO n_u-input and n_y-output plant $S(\mathbf{A}, \mathbf{B}, \mathbf{C})$ defined by

$$\mathbf{x}(k+1) = \mathbf{A}\mathbf{x}(k) + \mathbf{B}\mathbf{u}(k)q^{-d+1}, \quad \mathbf{x}(0) = \mathbf{x_0}, \tag{1a}$$

$$\mathbf{y}(k) = \mathbf{C}\mathbf{x}(k), \tag{1b}$$

with parameter matrices $\mathbf{A} \in \mathbb{R}^{n\times n}$, $\mathbf{B} \in \mathbb{R}^{n\times n_u}$, $\mathbf{C} \in \mathbb{R}^{n_y\times n}$, where symbols n, n_u and n_y express the numbers of $\mathbf{x}(k)$-state, $\mathbf{u}(k)$-input and $\mathbf{y}(k)$-output variables, respectively, whilst $\mathbf{x_0}$ denotes an initial condition of the state vector $\mathbf{x}(k)$. Next k stands for the discrete time, whereas d indicates the time delay of an analyzed system.

The perfect control formula minimizing the norm

$$J_u = \|\mathbf{y}(k+d) - \mathbf{y_{ref}}(k+d)\|^2, \tag{2}$$

engaging the n_y-vectors $\mathbf{y}(k+d)$ and $\mathbf{y_{ref}}(k+d)$ as the respective d-step deterministic output predictor and arbitrary reference value, sounds as follows

$$\mathbf{u}(k) = (\mathbf{CB})^{\mathrm{R}}[\mathbf{y_{ref}}(k+d) - \mathbf{C}(\sum_{i=1}^{d-1}\mathbf{A}^i\mathbf{B}\mathbf{u}(k-i) + \mathbf{A}^d\mathbf{x}(k))]. \tag{3}$$

Observe, that the perfect control algorithm (3) guarantees $\mathbf{y}(k) = \mathbf{y_{ref}}(k)$ for $k \geq d$.

Note that symbol $(.)^{\mathrm{R}}$ indicates some nonunique right inverse, including the regular one $(.)^{-1}$, of the $(n_y \times n_u)$-$\mathbf{CB}$ matrix product. For left-invertible systems $(n_y > n_u)$ the such IMC algorithm certainly does not exist, so far.

Remark 1: The IMC laws (3) *can recursively be calculated according to the formulas* (1) *for each time delay d.*

Remark 2: From plethora of inverses we consume the recently introduced polynomial matrix σ-inverse in the form of

$$\underline{\mathbf{G}}^{\mathrm{R}}_{\sigma}(q^{-1}) = \underline{\beta}^{\mathrm{T}}(q^{-1})[\underline{\mathbf{G}}(q^{-1})\underline{\beta}^{\mathrm{T}}(q^{-1})]^{-1}, \tag{4}$$

which is associated with the infinite number of so-called degrees of freedom $\underline{\beta}(q^{-1})$. Henceforth, through the special selected degrees of freedom we can impact the energy and robustness properties of the multivariable perfect control inputs (3)*. Notice that for $\underline{\beta}(q^{-1}) = \underline{\mathbf{G}}(q^{-1})$ we receive the unique minimum-norm T-inverse [30]. Of course, for simplicity of conducted study, the instance of σ-inverse solely employing parameter DOFs is investigated.*

Consequently, there is a fundamental question covering the choice of the parameter $\underline{\beta}(q^{-1})$ matrix derived from the generalized σ-inverse (4), which guarantees the minimum-energy perfect control design. The answer to that issue, for the selected class of systems, is shown throughout this manuscript.

Having the preliminaries, let us present the main achievement of the manuscript in the subsequent sections.

IV. ENERGY PROBLEM FORMULATION

In order to formulate a new authors' approach, the definition of the perfect control energy under squared $\mathcal{L}_2$-norm has to be shown in the following manner

$$E_u^N = \sum_{k=0}^{N}\mathbf{u}^{\mathrm{T}}(k)\mathbf{u}(k), \tag{5}$$

where $\mathbf{u}(k)$ is defined by Eq. (3) and symbol N implies an arbitrary chosen time horizon.

Therefore, the performance index (5) considering the energy is equal to (w.l.o.g. we responsibly assume that $\mathbf{y_{ref}}(k) = \mathbf{0}$ and $d = 1$)

$$E_u^N = \sum_{k=0}^{N}[(\mathbf{CB})^{\mathrm{R}}\mathbf{CAx}(k)]^{\mathrm{T}}[(\mathbf{CB})^{\mathrm{R}}\mathbf{CAx}(k)]. \tag{6}$$

A. TOWARDS A GENERAL THEORY OF MINIMUM-ENERGY PERFECT CONTROL DESIGN

At the same time, after substitution the Eq. (3) into formula (1a) we arrive at the relation significant for further investigation as follows

$$\mathbf{x}(k+1)=\mathbf{F}\mathbf{x}(k), \tag{7}$$

where $\mathbf{F}=[(\mathbf{I_n}-\mathbf{B}(\mathbf{CB})^{\mathrm{R}}\mathbf{C})\mathbf{A}]$ and $\mathbf{I_n}$ stands for the n-identity matrix.

Thus, the aforementioned expression can successfully be rewritten to the substantial operator form

$$z\left(\mathbf{X}(z)-\mathbf{X}(0)\right)=\mathbf{F}\mathbf{X}(z), \tag{8}$$

with symbol z representing the complex variable.

Hence, after simple manipulations we gain

$$(z\mathbf{I_n}-\mathbf{F})\mathbf{X}(z)=z\mathbf{X}(0), \tag{9}$$

which represents the closed-loop perfect control system behavior.

Considering the achieved results, an essential theorem supported by adequate lemma should immediately be formulated in the following way.

Lemma 1: Any solution to the equation $\mathbf{Ax}=\mathbf{b}$ *can be expressed as the sum of fixed outcome* $\mathbf{v}$ *and an arbitrary element of the kernel of* $\mathbf{A}$*. Thus, the solution set* $\mathbf{x}$ *to the equation* $\mathbf{Ax}=\mathbf{b}$ *fulfills*

$$\{\mathbf{v}+\mathbf{p}\mid \mathbf{Av}=\mathbf{b}\wedge\mathbf{p}\in\ker(\mathbf{A})\}. \tag{10}$$

After taking into account the expression (10) incorporated into formula (9) we arrive at the fundamental relation

$$\mathbf{p}\in\ker(z\mathbf{I_n}-\mathbf{F}), \tag{11}$$

where vector $\mathbf{p}$ corresponds to the z-operator-oriented multivariable plant (9).

Theorem 1: Consider the second-order MISO system governed by Eqs. (1)*. Then, for any initial condition* $\mathbf{x_0}$*, the* $\mathbf{x}(1)$ *always lies in the kernel of* $(z_{\mathbb{R}}\mathbf{I_2}-\mathbf{F})$*, that is*

$$\mathbf{x}(1)\in\ker(z_{\mathbb{R}}\mathbf{I_2}-\mathbf{F}), \tag{12}$$

where $z_{\mathbb{R}}$ *is a single-nonzero pole of the closed-loop perfect control system* (7)*.*

Proof: Observe, that the second-order MISO system defined by expression (7) commonly possesses two eigenvalues as follows

$$\operatorname{eig}(\mathbf{F})=\{z_{\mathbb{R}},0\}, \tag{13}$$

since the matrix $\mathbf{F}$ is always singular under perfect control consideration.

Thus, in order to fulfill the Theorem (1) the subsequent new relation has to be approved

$$(z_{\mathbb{R}}\mathbf{I_2}-\mathbf{F})\mathbf{x}(1)=\mathbf{0}, \tag{14}$$

which immediately should be rewritten to the form

$$(z_{\mathbb{R}}\mathbf{F}-\mathbf{FF})\mathbf{x_0}=\mathbf{0}. \tag{15}$$

Next, the matrix $\mathbf{F}$ can be represented by the Jordan normal form in the following manner

$$\mathbf{F}=\mathbf{DJD}^{-1}, \tag{16}$$

with appropriate matrix $\mathbf{D}$ and

$$\mathbf{J}=\begin{bmatrix} z_{\mathbb{R}} & 0\\ 0 & 0\end{bmatrix}. \tag{17}$$

In such a way, the formula (15) can be specified as

$$(z_{\mathbb{R}}\mathbf{DJD}^{-1}-\mathbf{DJD}^{-1}\mathbf{DJD}^{-1})\mathbf{x_0}=\mathbf{0}, \tag{18}$$

or rather

$$(\mathbf{D}\begin{bmatrix} z_{\mathbb{R}}^2 & 0\\ 0 & 0\end{bmatrix}\mathbf{D}^{-1}-\mathbf{D}\begin{bmatrix} z_{\mathbb{R}}^2 & 0\\ 0 & 0\end{bmatrix}\mathbf{D}^{-1})\mathbf{x_0}=\mathbf{0}. \tag{19}$$

Finally, the last relation holds for any $\mathbf{x_0}$, which ends the proof. □

Remark 3: Naturally, for second zero-related eigenvalue we receive a trivial solution.

Pursuing the new energy-oriented approach, a necessary theorem has to be stated.

Theorem 2: Consider the second-order MISO system governed by Eqs. (1)*. Then, the* $\mathbf{x}(k)$ *for* $k\geq 1$ *lies in the kernel of* $(z_{\mathbb{R}}\mathbf{I_2}-\mathbf{F})$*, finally to obtain*

$$\mathbf{x}(k)\in\ker(z_{\mathbb{R}}\mathbf{I_2}-\mathbf{F}),\quad k\geq 1. \tag{20}$$

Proof: Immediately, after combining the formula (7) and Theorem (1). Revised expression (14) in form of

$$(z_{\mathbb{R}}\mathbf{I_2}-\mathbf{F})\mathbf{F}(\mathbf{F}^{\Psi}\mathbf{x_0})=\mathbf{0},\quad \Psi\geq 0, \tag{21}$$

ends the proof. □

Henceforth, in accordance with Theorem (2), our structure $\mathbf{x}(k)$ fulfills the statement (11) for $k\geq 1$, giving rise to define a crucial relation covering the second-order MISO plants as follows

$$(\mathbf{F}-z_{\mathbb{R}}\mathbf{I_2})\mathbf{x}(k)=\mathbf{0},\quad k\geq 1, \tag{22}$$

for any $\mathbf{x_0}$.

Furthermore, the Eq. (22) can be rewritten to the form

$$\mathbf{F}\mathbf{x}(k)=z_{\mathbb{R}}\mathbf{x}(k),\quad k\geq 1, \tag{23}$$

and finally, after occupation of peculiarity derived from formula (7), can be given as

$$\mathbf{x}(k+1)=z_{\mathbb{R}}\mathbf{x}(k),\quad k\geq 1. \tag{24}$$

Let us switch now to the breakthrough of the manuscript regarding the analytical issue of minimum-energy perfect control design for MISO systems.

B. MINIMUM-ENERGY PERFECT CONTROL NEW OUTCOME FOR MULTI-INPUT/SINGLE-OUTPUT PLANTS

Reflecting on the aforementioned study, our $d = 1$-originated perfect control law (3) expressed as

$$\mathbf{u}(k+1) = -(\mathbf{CB})^{\mathbf{R}}\mathbf{CAx}(k+1), \tag{25}$$

can be rewritten in accordance with the relation (24) to the form

$$\mathbf{u}(k+\xi) = -(\mathbf{CB})^{\mathbf{R}}\mathbf{CA}z_{\mathbb{R}}^{\xi}\mathbf{x}(k), \quad k \geq 1, \quad \xi = 0, 1, 2, \ldots \tag{26}$$

Thus, the total energy (5) can successfully be redefined to the following equation

$$E_u^N = E_u^0 + \sum_{k=1}^{N} E_u^{(k,1)}\Theta^{k-1}, \tag{27}$$

with $\Theta = z_{\mathbb{R}}^2$ and $E_u^{(k,1)} = \mathbf{u}^{\mathrm{T}}(1)\mathbf{u}(1)$.

Therefore, after assuming the properties of geometric sequence and perfect control stability behavior ($\Theta < 1$), the Eq. (27) can again be established as follows

$$E_u^N = E_u^0 + E_u^{(k,1)}\frac{1-\Theta^N}{1-\Theta}, \tag{28}$$

which for $N \to +\infty$ leads to the important new relation

$$E_u^{+\infty} = E_u^0 + E_u^{(k,1)}\frac{1}{1-\Theta}. \tag{29}$$

It should be noticed that the energy-based approach as in Eq. (29) dedicated to second-order MISO perfect control plants is a new idea never seen before. The theory allows to examine the complex minimum-energy control problem in a simple way, especially in terms of selection of proper degrees of freedom of recently introduced generalized σ-inverse. This peculiarity is shown in the next section.

At the end of this section, let us try to define some essential statements.

Theorem 3: The single-nonzero pole of the closed-loop perfect control systems can be calculated according to the formula

$$z_{\mathbb{R}} = \mathrm{Tr}(\mathbf{F}). \tag{30}$$

Proof: Immediately, after employing the well-known formula

$$\sum eig(\mathbf{F}) = \mathrm{Tr}(\mathbf{F}). \tag{31}$$

□

Conjecture 1: In order to obtain a single-nonzero pole of the closed-loop perfect control system, the following condition must be preserved

$$n - n_y = 1. \tag{32}$$

Next section summarizes the advantage of minimum-energy-oriented new issues.

V. MINIMUM-ENERGY PERFECT CONTROL DESIGN

In order to obtain the MISO minimum-energy performance (5) of our perfect control expression, the proper $\underline{\beta}(q^{-1})$ of the generalized inverse (4) should analytically be calculated. The appropriate solution of such problem would be understood in terms of providing the following relation

$$\frac{d\{E_u^{+\infty}\}}{d\{\underline{\beta}(q^{-1})\}} = \mathbf{0}. \tag{33}$$

Notwithstanding, the analytical result of this statement does not exist, so far, since, according to the formula (5), we receive

$$\frac{d\left\{\sum_{k=0}^{+\infty}\mathbf{u}^{\mathrm{T}}(k)\mathbf{u}(k)\right\}}{d\{\underline{\beta}(q^{-1})\}} = \mathbf{0}. \tag{34}$$

Observe, that the relation (34) involves the unsolvable analytical derivative operation of matrix by vector. Moreover, the infinity time horizon additionally precludes the minimum-energy perfect control design. In such a case, the Eq. (29), along with the entire associated machinery, will be appreciated here. After fusion of mainly expressions (29) and (5) as well as (30), under application of the σ-inverse having parameter-derived DOFs of β, the reduced scalar-related form of the relation (33) is rising as follows

$$\frac{d\{E_u^{+\infty}\}}{d\{\beta\}} = \begin{cases} \dfrac{\partial\{E_u^{+\infty}\}}{\partial\{\beta_1\}} = 0 \\ \dfrac{\partial\{E_u^{+\infty}\}}{\partial\{\beta_2\}} = 0 \\ \vdots \\ \dfrac{\partial\{E_u^{+\infty}\}}{\partial\{\beta_{n_u}\}} = 0. \end{cases} \tag{35}$$

Of course, $E_u^{+\infty}$ is now determined as in Eq. (29) with vector β of form

$$\beta = \begin{bmatrix}\beta_1 & \beta_2 & \ldots & \beta_{n_u}\end{bmatrix}. \tag{36}$$

Thus, the formulas (35) can now be rewritten to the following relations

$$\frac{d\{E_u^{+\infty}\}}{d\{\beta\}} = \begin{cases} L_1(\mathbf{A}, \mathbf{B}, \mathbf{C}, \beta, \mathbf{x_0}) = 0 \\ L_2(\mathbf{A}, \mathbf{B}, \mathbf{C}, \beta, \mathbf{x_0}) = 0 \\ \quad\vdots \\ L_{n_u}(\mathbf{A}, \mathbf{B}, \mathbf{C}, \beta, \mathbf{x_0}) = 0, \end{cases} \tag{37}$$

under plant condition

$$\frac{\partial\{E_u^{+\infty}\}}{\partial\{\beta_i\}} = \frac{L_i(\mathbf{A}, \mathbf{B}, \mathbf{C}, \beta, \mathbf{x_0})}{M_i(\mathbf{A}, \mathbf{B}, \mathbf{C}, \beta, \mathbf{x_0})}, \quad i = 1, 2, \ldots, n_u. \tag{38}$$

Observe, that all formulas $L_i(\mathbf{A}, \mathbf{B}, \mathbf{C}, \beta, \mathbf{x_0}) = 0$ correspond to the general equation

$$a_i{\beta_i}^4 + b_i{\beta_i}^3 + c_i{\beta_i}^2 + d_i\beta_i + e_i = 0, \tag{39}$$

arranging roots in forms of

$$\beta_{1i,2i} = -\frac{b_i}{4a_i} - S \pm \frac{1}{2}\sqrt{-4S^2 - 2p + \frac{q}{S}}, \quad (40)$$

$$\beta_{3i,4i} = -\frac{b_i}{4a_i} + S \pm \frac{1}{2}\sqrt{-4S^2 - 2p - \frac{q}{S}}, \quad (41)$$

where

$$p = \frac{8a_ic_i - 3b_i^2}{8a_i^2}, \quad (42)$$

$$q = \frac{b_i^3 - 4a_ib_ic_i + 8a_i^2d_i}{8a_i^3}, \quad (43)$$

$$S = \frac{1}{2}\sqrt{-\frac{2}{3}p + \frac{1}{3a_i}\left(Q + \frac{\Delta_0}{Q}\right)}, \quad (44)$$

$$Q = \sqrt[3]{\frac{\Delta_1 + \sqrt{\Delta_1^2 - 4\Delta_0^3}}{2}}, \quad (45)$$

$$\Delta_0 = c_i^2 - 3b_id_i + 12a_ie_i, \quad (46)$$

$$\Delta_1 = 2c_i^3 - 9b_ic_id_i + 27b_i^2e_i + 27a_id_i^2 - 72a_ic_ie_i. \quad (47)$$

Remark 4: It should be mentioned that the coefficients (a_i, b_i, c_i, d_i and e_i) from Eq. (39) *can analytically be calculated also under symbolic manner. However, due to the fact that they employ a number of components, we throw away this computational burden approach.*

Of course, in order to find the solution sets of expressions (37), we have to take into account the Hessian matrix associated with the second-order partial derivatives. This operation will be explained in details in the next unit.

Thus, for the purpose of confirmation of the entire new machinery, let us switch now to the numerical example.

VI. SIMULATION EXAMPLE

Consider a two-input one-output LTI discrete-time second-order system defined by the formulas (1) with $\mathbf{A} = \begin{bmatrix} 0.671497133608081 & -1.207486922685038 \\ 0.717238651328838 & 1.630235289164729 \end{bmatrix}$, $\mathbf{B} = \begin{bmatrix} 0.488893770311789 & 1.034693009917860 \\ 0.726885133383238 & -0.303440924786016 \end{bmatrix}$, $\mathbf{C} = \begin{bmatrix} 0.293871467096658 & -0.787282803758638 \end{bmatrix}$ and $\mathbf{x_0} = \begin{bmatrix} 5 \\ -3 \end{bmatrix}$. After applying the minimum-norm right T-inverse to the product of **CB** we obtain the total energy of the perfect control inputs equal to $E_u^{1000} = 410.9253$ according to the formulas (5) and (29). The signal runs of the state and control variables are presented in Figs. 1 and 2, respectively.

On the other hand, the engagement of the σ-inverse with $\beta = \begin{bmatrix} \beta_1 & \beta_2 \end{bmatrix}$ provides the Eq. (37)-oriented formulas

$$a_1\beta_1^4 + b_1\beta_1^3 + c_1\beta_1^2 + d_1\beta_1 + e_1 = 0, \quad (48)$$

$$a_2\beta_2^4 + b_2\beta_2^3 + c_2\beta_2^2 + d_2\beta_2 + e_2 = 0, \quad (49)$$

with coefficients of the polynomials in β-domain being in relation with the $\mathbf{A}$, $\mathbf{B}$, $\mathbf{C}$, β and $\mathbf{x_0}$.

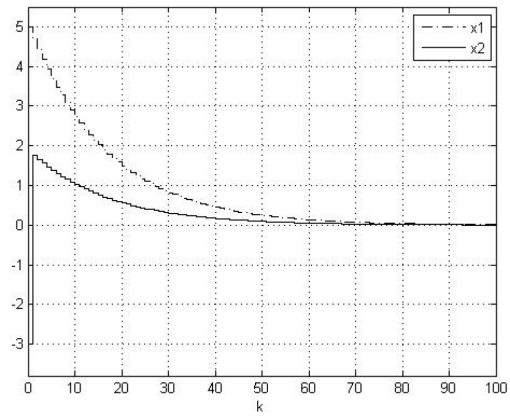

FIGURE 1. Perfect control: signals of x(k), T-inverse.

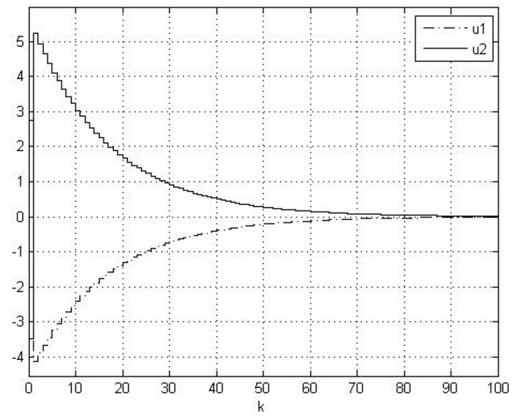

FIGURE 2. Perfect control: signals of u(k), T-inverse.

In should be emphasized, that the formulas (48) and (49) are interchangeable in context of application of the respective solution sets derived from both of them. Henceforth, the relations are linearly dependent. For instance, for arbitrary selected β_2 we arrive at

$$a_{11}\beta_1^4 + b_{11}\beta_1^3 + c_{11}\beta_1^2 + d_{11}\beta_1 + e_{11} = 0, \quad (50)$$

under coefficients $a_{11}, b_{11}, c_{11}, d_{11}$ and e_{11} strictly come from $\mathbf{A}$, $\mathbf{B}$, $\mathbf{C}$, β_2 and $\mathbf{x_0}$.

Therefore, for exemplary parametrized $\beta_2 = 2$, the four roots of Eq. (50), which can also be easily obtained through formulas (40) and (41), sound as follows

$$\begin{cases} \beta_{11} = -0.3057 + 0.8315i \\ \beta_{12} = -2.7610 \\ \beta_{13} = 5.2859 \\ \beta_{14} = -0.3057 - 0.8315i. \end{cases} \quad (51)$$

Of course, the roots equal to β_{11} and β_{14} should be omitted, as we operate in the discrete-time framework only.

Finally, in order to find the global minimum of the perfect control energy function, we have to apply the well-known paradigm of second-order derivative in the following manner

$$\frac{\partial^2 E_u^{+\infty}}{\partial \beta_1^2}|_{\beta_{12}} = 42.250, \quad (52)$$

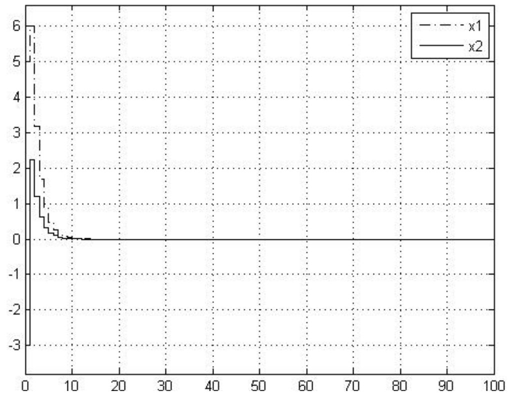

FIGURE 3. **Perfect control: signals of x(k), σ-inverse.**

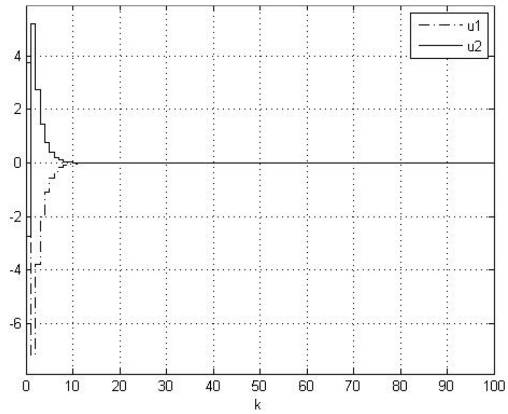

FIGURE 4. **Perfect control: signals of u(k), σ-inverse.**

$$\frac{\partial^2 E_u^{+\infty}}{\partial \beta_1^2}|_{\beta_{13}} = -34.936. \tag{53}$$

Thus, based on

$$\frac{\partial^2 E_u^{+\infty}}{\partial \beta_1^2}|_{\beta_i} > 0, \tag{54}$$

we immediately receive

$$\beta_{opt} = \begin{bmatrix} -2.7610 & 2 \end{bmatrix}. \tag{55}$$

Concluding, after application of σ-inverse with β_{opt} to the **CB** product we arrive at the single-nonzero pole of the closed-loop perfect control system equal to $z_{\mathbb{R}} = 0.5314$, with energy of the control input variables equals $E_{u_{opt}}^{1000} = 129.9853$ (calculated according to Eq. (29)). The respective signal runs of the state and control vectors are depicted in Figs. 3 and 4.

Corollary 1: It is remarkable, that analytically appointed optimal degrees of freedom β_{opt} of the σ-inverse guarantee the minimum-energy perfect control design. Amazingly, from now on, the T-inverse can not be treated as the 'best' one in terms of the energy expenditure of the perfect control input variables, in general.

Remark 5: It should be strongly emphasized, that the entire computational effort can be done for any $\beta_2 \in \mathbb{R}^{1\times n_u} \setminus \{\mathbf{0}\}$, as the statement occurs $\beta_1 = \gamma\beta_2$, where $\gamma(\mathbf{A}, \mathbf{B}, \mathbf{C}, \mathbf{x_0})$ is a certain function. Moreover, for every β_2 we obtain a different β_{opt}, which finally preserves the same value of $E_{u_{opt}}$, in each scenario.

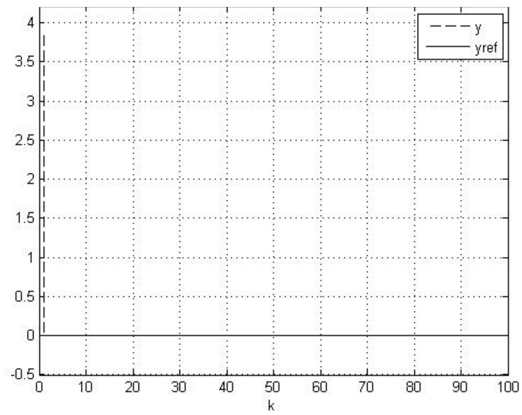

FIGURE 5. **Perfect control: $y(k)$ and $y_{ref}(k)$ signals, both cases.**

It is symptomatic, that dumping plots of $\mathbf{u}(k)$ and $\mathbf{x}(k)$ signals are running for $k \geq 1$ with decreasing impact equal to $z_{\mathbb{R}} = 0.5314$. This fact is additionally confirmed by newly introduced expression (24). Naturally, the perfect control output remains at the reference/setpoint $y(k) = 0$ for $k \geq 1$ (see Fig. (5)).

VII. CONCLUSIONS AND OPEN PROBLEMS

The original observation covering the minimum-energy perfect control design problem is proposed in this paper. Based on the new issue, we can solve in a simple way the energy-related task for the special class of the state-space systems. The given theory certainly leads to the clarification of such complex mathematical perfect control-oriented peculiarity. It is clear now that the σ-inverse outperforms the T-inverse in terms of the energy expenditure of the perfect control input variables, which has been confirmed in analytical manner. Due to the fact, that the presented material constitutes still unexplored research area, we can formulate an accompanying series of open problems. The two most important subjects should be recalled at the moment. Firstly, it would be interesting to extend the new geometric approach to cover the state-space plants having nonzero reference value $\mathbf{y_{ref}}(k)$ and more than one nonzero closed-loop perfect control pole. Secondly, the synthesis of the systems with $d > 1$ should establish an important factor allowing to ultimately formulate the general theory of minimum-energy perfect control design. In the end, the validation of the new postulated methodology by the practical implementation is still waiting for further consideration.

REFERENCES

[1] W. P. Hunek and P. Majewski, "Perfect reconstruction of signal—A new polynomial matrix inverse approach," *EURASIP J. Wireless Commun. Netw.*, vol. 2018, no. 1, p. 107, May 2018, doi: 10.1186/s13638-018-1122-5.

[2] W. P. Hunek and P. Dzierwa, "New results in generalized minimum variance control of computer networks," *Inf. Technol. Control*, vol. 43, no. 3, pp. 315–320, Sep. 2014, doi: 10.5755/j01.itc.43.3.6268.

[3] W. P. Hunek and T. Feliks, "A geometric-based approach to the maximum-speed state and output variables for some class of IMC structures," in *Proc. 6th Int. Conf. Control, Decis. Inf. Technol. (CoDIT)*, Paris, France, Apr. 2019, pp. 1385–1389, doi: 10.1109/CoDIT.2019.8820536.

[4] W. P. Hunek, D. Paczko, T. Feliks, and M. Krok, "A norm-based approach to the minimum-energy multivariable perfect control design," in *Proc. 22nd Int. Conf. Syst. Theory, Control Comput. (ICSTCC)*, Sinaia, Romania, Oct. 2018, pp. 7–11, doi: 10.1109/ICSTCC.2018.8540653.

[5] A. Ben-Israel and T. Greville, *Generalized Inverses: Theory and Applications*. New York, NY, USA: Springer, 2006.

[6] H. L. Trentelman, A. A. Stoorvogel, and M. Hautus, *Control Theory for Linear Systems* (Communications and Control Engineering). New York, NY, USA: Springer-Verlag, 2001.

[7] T. Kaczorek, A. Dzieliński, W. Dąbrowski, and R. Łopatka, *Fundamentals of Control Theory*, 3rd ed. Warsaw, Poland: WNT, 2009.

[8] S. Dadhich and W. Birk, "Analysis and control of an extended quadruple tank process," in *Proc. Eur. Control Conf. (ECC)*, Strasbourg, France, Jun. 2014, pp. 838–843, doi: 10.1109/ECC.2014.6862290.

[9] T. Zhang, H. G. Li, Z. Y. Zhong, and G. P. Cai, "Hysteresis model and adaptive vibration suppression for a smart beam with time delay," *J. Sound Vib.*, vol. 358, pp. 35–47, Dec. 2015, doi: 10.1016/j.jsv.2015.08.017.

[10] T. Zhang, H. G. Li, and G. P. Cai, "Hysteresis identification and adaptive vibration control for a smart cantilever beam by a piezoelectric actuator," *Sens. Actuators A, Phys.*, vol. 203, pp. 168–175, Dec. 2013, doi: 10.1016/j.sna.2013.08.042.

[11] T. Zhang, B. T. Yang, H. G. Li, and G. Meng, "Dynamic modeling and adaptive vibration control study for giant magnetostrictive actuators," *Sens. Actuators A, Phys.*, vol. 190, pp. 96–105, Feb. 2013, doi: 10.1016/j.sna.2012.11.001.

[12] M. J. G. Silva, C. S. Araujo, S. T. M. Bezerra, C. R. Souto, S. A. Silva, and H. P. Gomes, "Generalized minimum variance control for water distribution system," *IEEE Latin Amer. Trans.*, vol. 13, no. 3, pp. 651–658, Mar. 2015, doi: 10.1109/TLA.2015.7069088.

[13] A. Zhakatayev, M. Rubagotti, and H. A. Varol, "Closed-loop control of variable stiffness actuated robots via nonlinear model predictive control," *IEEE Access*, vol. 3, pp. 235–248, 2015, doi: 10.1109/ACCESS.2015.2418157.

[14] E. Atam, L. Mathelin, and L. Cordier, "Identification-based closed-loop control strategies for a cylinder wake flow," *IEEE Trans. Control Syst. Technol.*, vol. 25, no. 4, pp. 1488–1495, Jul. 2017, doi: 10.1109/TCST.2016.2604779.

[15] X. Gong, Y. Wang, H. Chen, and Y. Hu, "Double closed-loop controller design for boost pressure control of turbocharged gasoline engines," *IEEE Access*, vol. 7, pp. 97333–97342, 2019, doi: 10.1109/ACCESS.2019.2928856.

[16] D. Wang, A. Wang, Y. Fu, J. Xiao, and H. Liu, "Robust nonlinear perfect control for semiconductor refrigeration device," in *Proc. 10th Int. Conf. Softw., Knowl., Inf. Manage. Appl. (SKIMA)*, Chengdu, China, 2016, pp. 413–417, doi: 10.1109/SKIMA.2016.7916257.

[17] J.-R. Li and M.-G. Gan, "A novel robust perfect tracking control method for nonlinear servo systems," in *Proc. 37th Chin. Control Conf. (CCC)*, Wuhan, China, Jul. 2018, pp. 3790–3795, doi: 10.23919/ChiCC.2018.8482835.

[18] S.-H. Lee and C. C. Chung, "Reference redesigned perfect tracking control, with application to servo control system," in *Proc. 53rd IEEE Conf. Decis. Control*, Los Angeles, CA, USA, Dec. 2014, pp. 4542–4547, doi: 10.1109/CDC.2014.7040098.

[19] P. Yang, X. Zhou, H. Guo, and Y. Zhou, "Research on self-turning minimum variance control algorithm in non-minimum phase system," in *Proc. IEEE 15th Int. Conf. Netw., Sens. Control (ICNSC)*, Zhuhai, China, Mar. 2018, pp. 1–5, doi: 10.1109/ICNSC.2018.8361273.

[20] W. Yunjie, W. Junfeng, L. Xiaodong, and T. Dapeng, "A new control method with perfect tracking control for flight simulator," in *Proc. Chin. Control Decis. Conf. (CCDC)*, Mianyang, China, May 2011, pp. 2571–2576, doi: 10.1109/CCDC.2011.5968644.

[21] S.-H. Hur and M. J. Grimble, "Robust nonlinear generalised minimum variance control and fault monitoring," *Int. J. Control, Automat. Syst.*, vol. 13, no. 3, pp. 547–556, Mar. 2015.

[22] D. Horla, "Minimum variance adaptive control of a servo drive with unknown structure and parameters," *Asian J. Control*, vol. 15, no. 1, pp. 120–131, Dec. 2011, doi: 10.1002/asjc.479.

[23] X.-H. Chang, J. H. Park, and J. Zhou, "Robust static output feedback H∞ control design for linear systems with polytopic uncertainties," *Syst. Control Lett.*, vol. 85, pp. 23–32, Nov. 2015, doi: 10.1016/j.sysconle.2015.08.007.

[24] X.-H. Chang, Q. Liu, Y.-M. Wang, and J. Xiong, "Fuzzy peak-to-peak filtering for networked nonlinear systems with multipath data packet dropouts," *IEEE Trans. Fuzzy Syst.*, vol. 27, no. 3, pp. 436–446, Mar. 2019, doi: 10.1109/TFUZZ.2018.2859903.

[25] X. Zhao, X. Zheng, C. Ma, and R. Li, "Distributed consensus of multiple Euler–Lagrange systems networked by sampled-data information with transmission delays and data packet dropouts," *IEEE Trans. Autom. Sci. Eng.*, vol. 14, no. 3, pp. 1440–1450, Jul. 2017, doi: 10.1109/TASE.2015.2448934.

[26] W. Hunek and K. Latawiec, "A study on new right/left inverses of nonsquare polynomial matrices," *Int. J. Appl. Math. Comput. Sci.*, vol. 21, no. 2, pp. 331–348, Jun. 2011, doi: 10.2478/v10006-011-0025-y.

[27] W. P. Hunek, "New SVD-based matrix H-inverse vs. minimum-energy perfect control design for state-space LTI MIMO systems," in *Proc. 20th Int. Conf. Syst. Theory, Control Comput. (ICSTCC)*, Sinaia, Romania, Oct. 2016, pp. 14–19, doi: 10.1109/icstcc.2016.7790633.

[28] L. Noueili, W. Chagra, and M. Ksouri, "New iterative learning control algorithm using learning gain based on σ inversion for nonsquare multi-input multi-output systems," *Model. Simul. Eng.*, vol. 2018, pp. 1–9, Jun. 2018, doi: 10.1155/2018/4195938.

[29] W. P. Hunek and M. Krok, "Pole-free perfect control for nonsquare LTI discrete-time systems with two state variables," in *Proc. 13th IEEE Int. Conf. Control Automat. (ICCA)*, Ohrid, Macedonia, Jul. 2017, pp. 329–334, doi: 10.1109/ICCA.2017.8003082.

[30] W. P. Hunek, "Perfect control for right-invertible Grünwald–Letnikov plants—An innovative approach to practical implementation," *Fractional Calculus Appl. Anal.*, vol. 22, no. 2, pp. 424–443, Apr. 2019, doi: 10.1515/fca-2019-0026.

WOJCIECH PRZEMYSŁAW HUNEK received the Ph.D. and Habilitation degrees in electrical engineering and automatic control and robotics from the Faculty of Electrical, Control and Computer Engineering, Opole University of Technology, in 2003 and 2012, respectively. He holds the post of the Deputy Dean of education at the Faculty of Electrical, Control and Computer Engineering. He works as an Associate Professor at the Institute of Control Engineering. He is also the Head of the Control Systems and Industrial Automation Team. He has authored or coauthored about 100 articles, most of which are concerned with the up-to-date topics in multivariable control and systems theory.

TOMASZ FELIKS was born in 1992. He received the master's degree in control and robotics from the Department of Electrical, Control and Computer Engineering, Opole University of Technology, in 2017, where he is currently pursuing the Ph.D. degree. His research interest is focused on the minimum-energy control problems.